

Heavy Quark dynamics in the Quark-Gluon Plasma

Vincenzo Greco^{*†}

Department of Physics and Astronomy, University of Catania, Via S. Sofia 64, 95125 Catania, Italy

Laboratori Nazionali del Sud, INFN-LNS, Via S. Sofia 62, I-95123 Catania, Italy

E-mail: greco@lns.infn.it

Francesco Scardina, Santosh Kumar Das, Salvatore Plumari

Department of Physics and Astronomy, University of Catania, Via S. Sofia 64, 95125 Catania, Italy

Laboratori Nazionali del Sud, INFN-LNS, Via S. Sofia 62, I-95123 Catania, Italy

E-mail: scardinaf@lns.infn.it, sdas@lns.infn.it, plumari@ct.infn.it

In this talk we review the basic concepts related with the study of the dynamics of the heavy quarks in the quark-gluon plasma created in ultra-relativistic heavy-ion collisions. We discuss the relevant physical scale as well the difficulties of the present theoretical approach to have a self-consistent description of the experimental data at both RHIC and LHC. In the second part we challenge the assumption of brownian motion for charm quarks and compare the dynamical evolution of charm and bottom quarks in a Fokker-Planck approach and in a Transport Boltzmann one. We show that while for bottom the motion appears quite close to a Brownian one, this does not seem to be the case for charm quarks. In particular the solution of the full two-body collision integral shows that the anisotropic flows are larger respect to those predicted by a Langevin dynamics.

52 International Winter Meeting on Nuclear Physics - Bormio 2014,

27-31 January 2014

Bormio, Italy

^{*}Speaker.

[†]The authors acknowledge the support of the ERC-StG Grant under the project QGPDyn.

1. Introduction: specific features of Heavy Quarks in the QGP

One of the primary aims of the ongoing nuclear collisions at Relativistic Heavy Ion Collider (RHIC) and Large Hadron Collider (LHC) energies is to create a new state of matter where the bulk properties of the matter are governed by the light quarks and gluons [1, 2]. In this context, the heavy quarks (HQ) mainly charm and bottom quarks play a crucial role since they do not constitute the bulk part of the matter due to their larger mass respect to the temperature created in ultra-relativistic heavy-ion collisions (uRHIC's) [3]. This allows to have a kind of external probe respect to the bulk of the QGP medium that being affected by its density, temperature and collective expansion carry the information of the created plasma. HQ are therefore considered heavy for a two-fold reason: the first, typical of particles physics, is that the mass $M_Q \gg \Lambda_{QCD}$ which makes possible the evaluation of cross section and p_T spectra within next-to-next-to-lead order (N²LO) [4, 5] in a perturbative QCD (pQCD) scheme; the second more inherent to plasma physics is that $M_Q \gg T$ and therefore the thermal production in the QGP is expected to be negligible because it is suppressed approximately by a $\sim e^{-M/T}$ term. Hence for HQ one has a early exact flavor conservation during the evolution of the plasma in both the partonic and hadronic stages. This remains true going from SPS to LHC energies spanning a T range of $\sim 200 - 600$ MeV, as we can see in Fig.1 where the ratio M/T_{max} , with T_{max} the estimated maximum initial temperatures at different collider for SPS (diamonds), RHIC (circles) up to LHC (squares). We notice that even if the collision energy from SPS to RHIC goes up by about a factor 10^2 the maximum temperature increase by at most a factor of three leaving the ratio M/T for charm, bottom and quarks always quite large than one. In Fig.1 we have also indicated by a shaded area where the value of $M/T \sim 1/2$ is such that one can approximately expect that most of quarks are produce thermally and from this point of view can be considered light respect to the available energy. We notice that the strange quark s already at SPS energy is such to be mostly thermally created, which is naively the reason why there is a strange enhancement respect to pp collisions already at energies below the maximum SPS $\sqrt{s_N N} = 17.8 GeV$ [6].

Furthermore HQ are quite good probes of the QGP because they are produced in the very early stage of the collision, as their production is associated with Q^2 large momentum transfer, hence the production time $\tau_0^Q \ll \tau_{QGP}$ is much smaller that the QGP lifetime therefore HQ pass through the entire space-time evolution of the system and their thermal production and annihilation can be ignored being "heavy" respect to thermal excitations as discussed above.

A key issue also to understand the amount of information the study of HQ observables can provide is the thermalization time. In a pQCD framework, that was believed to be valid for c and b quarks, is estimated to be of the order of 10-15 fm/c for charm and about 25-30 fm/c for bottom [3, 9, 10, 11] for the temperature range relevant in for the QGP formed at RHIC and LHC. This means that one should not expect a full thermalization of HQ in uRHIC's, in fact the lifetime time of the QGP, τ_{QGP} , about 4-5 fm/c at RHIC and about 10-12 fm/c at LHC. This would mean $\tau_{th}^Q \geq \tau_{QGP} \gg \tau_{eq}^q$ and therefore the HQ would be more sensitive to the history of the QGP evolution at variance with the light quarks that thermalize in less than 1 fm/c and hence are less dependent on the details of their interaction. Indeed this could be the underlying reason of a fast success in the description of the momentum spectra distribution and collective flows for light hadrons, while as we will discuss a self-consistent description of the data in the heavy sector is still pending at both

RHIC and LHC energies.

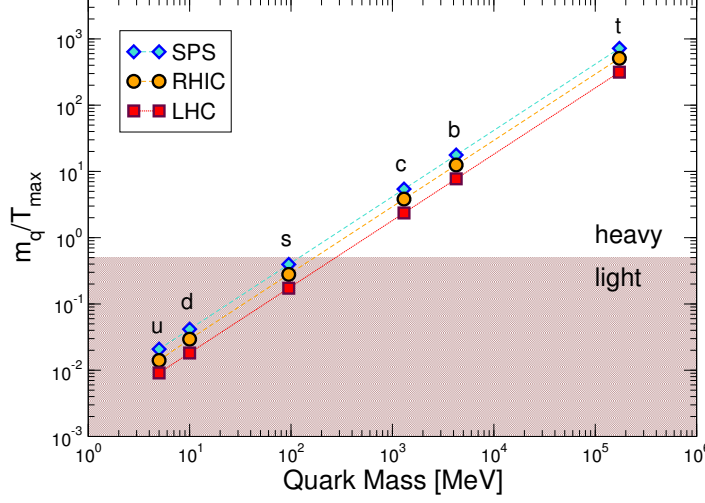


Figure 1: Ratio of the quark mass to the maximum temperature reached in heavy-ion collisions at SPS, RHIC and LHC.

The theoretical challenge is to understand the corresponding thermalization times of heavy quarks from the underlying microscopic scattering processes with the constituents of the QGP, in particular how the heavy quarks, despite their large masses, $m_Q \gg T_c$, become part of the collective flow of the fireball.

The $m_Q \gg T$ has two important implications of more theoretical nature still fundamental to make possible the comparison between the experimental data and the information coming from QCD solved on lattice. In fact, the large mass implies also that the momentum exchange by collisions $|q^2| \ll m_Q^2$ (parametrically dominated by elastic scatterings) and the dynamics can be treated as a Brownian motion by mean of a Fokker-Planck equation which constitutes a significant simplification of the study of the transport properties. Finally the three-momentum transfer dominates over energy transfer $|\vec{q}| \gg q_0 \sim \frac{\vec{q}^2}{m_Q}$ which parametrically makes possible the concept of a potential and therefore to link the HQ physics to the studies to of the heavy-quark free energy in lQCD [16], as we will discuss in the next Section.

We will discuss briefly early ideas about HQ quarks as a probe of the QGP emphasizing the difficulties in describing simultaneously the modification of they spectra respect to pp collisions and the large elliptic flow v_2 , a measure of the anisotropic flow, observed experimentally. In the second part we will focus on the theoretical approaches to describe the dynamical evolution of the HQ comparing the most commonly used Fokker-Planck approach to the Boltzmann transport equation. We discuss that while for the bottom quark the two approaches give very similar results for the charm quark both the nuclear suppression factor R_{AA} and the elliptic flow v_2 are larger going more closer to experimental observations.

2. Early Ideas on Heavy quarks in the QGP

There are presently two main observable related with heavy quarks that have been measured

at both RHIC and LHC energy. The first is the so-called nuclear suppression factor R_{AA} that is the ratio between the p_T momentum spectra in AA collisions and the p_T spectrum observed in pp collisions (rescaled by the number of collisions N_{coll}):

$$R_{AA}(p_T) = \frac{d^2N_{AA}/dp_T^2}{N_{coll} d^2N_{pp}/dp_T^2}$$

Therefore $R_{AA} = 1$ means that what is happening in a AA collisions is just superposition of pp collisions. For light quark it was clearly observed an $R_{AA} \sim 0.25$ indicating a strong quenching of the spectra in the QGP medium due to elastic collisions and mainly to in-medium gluon radiation. For HQ about a decade ago the expectations were for a perturbative interaction of HQ with the medium, hence due to the large mass respect to the light quarks and also to the energy scale set by the QGP temperature the predictions were a $R_{AA} \approx 0.6$ for charm quarks and $R_{AA} \approx 0.8 - 0.9$ for bottom quarks for central collisions [12, 13] at intermediate p_T . A sketch of such a prediction is depicted in Fig. 2.

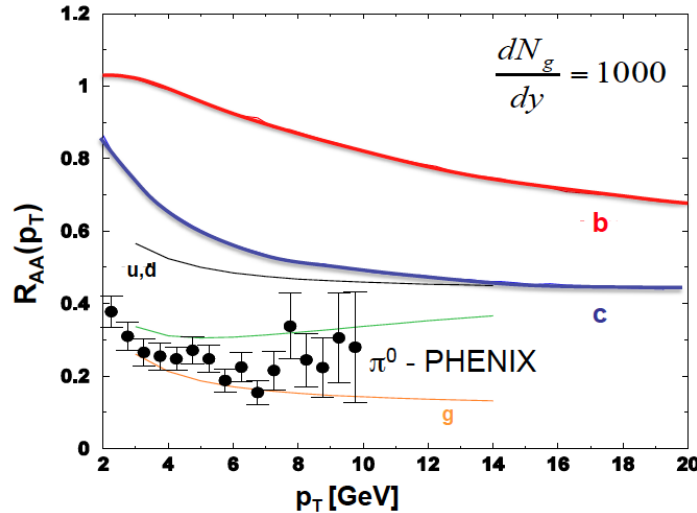


Figure 2: R_{AA} prediction for c and b quarks in Au+Au central collisions at $\sqrt{s_{NN}} = 200 AGeV$ according to a jet quenching mechanism of gluon radiation. The prediction for light quarks and gluons are also reported and compared to experimental data on π^0 by PHENIX. Figure adapted from [12].

The other key observable is the elliptic flow $v_2 = \langle \cos(2\phi_p) \rangle$, a measure of the anisotropy in the angular distribution that corresponds to the anisotropic emission of particles respect to the azimuthal angle according to the simple formula $N(\phi = 0^0)/N(\phi = 90^0) = (1 - 2v_2)/(1 + 2v_2)$, valid under the assumption that v_2 is the only anisotropy present. An important feature of relativistic heavy-ion collisions has been the observation of large values of the elliptic flow that in some kinematical region reaches value of about $\sim 0.2 - 0.25$, corresponding to about a factor 2-3 more particle at $\phi = 0^0$ respect to $\phi = 90^0$. For HQ about a decade ago the prediction was that they can acquire only a quite small $v_2 \sim 0.02$ respect to the light hadron ones [13]. Therefore the first experimental results hence came as a surprise showing a quite small $R_{AA}(p_T)$ similar to the pion one and a quite large $v_2(p_T)$ of single e^\pm coming from D and B mesons decay. The last were

in approximate agreement with a scenario of heavy quarks almost flowing with the bulk medium [14, 15]. This has of course even increased the interest for the understanding of the heavy flavor dynamics in the QGP.

There have been mainly two approaches to fill the gap between the prediction of a standard perturbative approach and the experimental data. One argues essentially that the screening in the HQ sector is quite smaller respect to the standard modeling $m_D \sim g(T)T$, where g is the strong running coupling. A reduced screening leads essentially to much larger cross section that leads to predict smaller R_{AA} respect to the first jet quenching one. A different approach take the point of view that in such approaches from pQCD, based on gluon-bremsstrahlung energy loss and/or including elastic HQ scattering, one has to artificially tune the coupling strength beyond the applicability range of perturbation theory. Indeed It has also been shown that the convergence of the perturbative series for the HQ diffusion coefficient is quite poor. Thus, non-perturbative approaches have to be used to explain the strong HQ couplings necessary. One suggested mechanism is the formation of D - and B - meson resonance excitations in the deconfined phase of QCD matter [10, 17] which has lead to a quite satisfactory description of the e^\pm coming from semileptonic decay of B and D meson at RHIC.

The idea of the existence of resonant scattering is supported by IQCD on both the quark correlators for both heavy and light quarks [19] showing the existence of a peak in the spectral function even at temperatures substantially higher than T_c suggesting the presence of physical mechanism beyond a simple free scattering.

The heavy quark mass as mentioned in the introduction allows the use of an interaction potential between quarks, this has the advantages to employ the T-matrix scattering theory which does not rely on a perturbative expansion. An extra benefit that arises is that one can in principle extract the quark potential from finite-temperature lattice QCD (IQCD), or at least be constrained by IQCD “data“ which gives a parameter-free input. On the other hand currently the main source of uncertainties is just the extraction of the potential from the lattice calculation on the free energy. We assume that the effective in-medium potential can be extracted from finite-temperature IQCD calculations of the color-singlet free energy $F_1(r, T)$ [20, 21] for a static $\bar{Q}Q$ pair as the internal potential energy by the usual thermodynamic relation [23, 24],

$$U_1(r, T) = F_1(r, T) - T \frac{\partial F_1(r, T)}{\partial T}. \quad (2.1)$$

For the details on the assumption behind such a choice one can refer to Ref.s [17]. However the successful application to compute quarkonium correlators and HQ susceptibilities lends a-posteriori support (albeit not validation) of the U choice. One generally also consider the complete set of color channels for the $Q\bar{q}$ (singlet and octet) and Qq (anti-triplet and sextet) systems, using Casimir scaling as in leading-order pQCD, $V_8 = -V_1/8$, $V_{\bar{3}} = V_1/2$, $V_6 = -V_1/4$, which is also justified by recent IQCD calculations of the finite- T HQ free energy [25].

We restrict ourselves to S ($l = 0$) and P ($l = 1$) waves. The main result is that in the dominating attractive color-singlet $Q\bar{q}$ and color-antitriplet Qq channels, close to the critical temperature, T_c , the T -matrix approach suggests the presence of resonance states. Such resonance states increase the strength of the interaction and naturally merge into a quark coalescence mechanism, as $T \rightarrow T_c$, dominated by the color-singlet state, while the scattering become quasi-free at $T \gtrsim 2T_c$. Therefore

while the free-scattering predicts a Drag of the HQ that goes down with the density of the bulk system $\rho_{bulk} \propto T^{-3}$, the resonant scattering tends to compensate the decrease by the density scatterers because takes into account that the attractive quark-potential becomes stronger close to the phase transition.

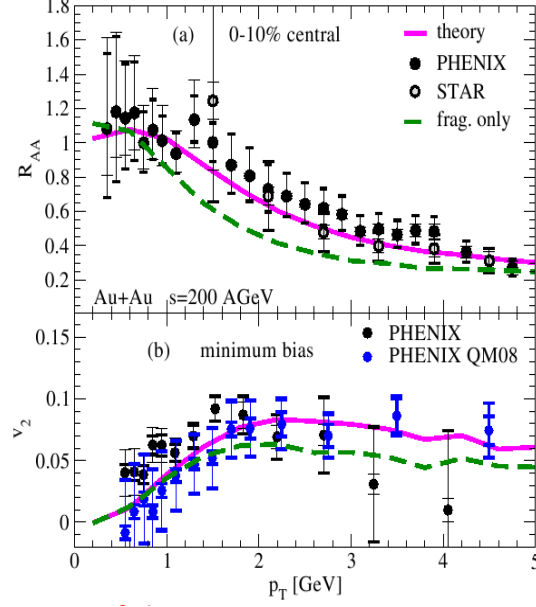


Figure 3: Nuclear Suppression factor R_{AA} (upper panel) for Au+Au at $\sqrt{s_{NN}} = 200$ AGeV and elliptic flow v_2 (lower panel). Data are compared to T-matrix model with hadronization by coalescence+ fragmentation (solid line) and only fragmentation (dashed line).

To compare with the experimental a Fokker-Planck approach has been used to described the motion of HQ in the expanding medium described by hydrodynamics, and finally a quark-coalescence model described in [26, 27] allows to take into account the hadronization that allow the comparison with the single-electron p_T data from RHIC of the HQ spectra to D - and B -mesons and their subsequent semileptonic decay to e^\pm . As shown in Fig. 3 the Langevin simulation of the HQ diffusion, followed by the combined quark-coalescence fragmentation description of hadronization to D and B mesons and their subsequent semileptonic decay, successfully accounts simultaneously for both the R_{AA} and v_2 of single electrons in 200 AGeV Au-Au collisions [28, 29] at RHIC. Comparing the solid and dashed lines one can see the effects from the “momentum kick” of the light quarks in quark coalescence, an enhancement of both, R_{AA} and v_2 , is important for the quite good agreement of both observables with the data.

A closer inspection of the time evolution of the p_T spectra shows that the suppression of high- p_T heavy quarks occurs mostly in the beginning of the time evolution, while the v_2 is built up later at temperatures close to T_c which is to be expected since the v_2 of the bulk medium is fully developed at later stages only [30]. This effect is more pronounced due to resonance formation because the transport coefficients become larger close to T_c or anyway decrease much slower than the pQCD case.

Therefore a resonance model supplemented by a coalescence mechanism seems to be able to describe the data at RHIC. However, all approaches show some difficulties to predict correctly both $R_{AA}(p_T)$ and $v_2(p_T)$ and such a trait is present not only at RHIC energy (where there is the uncertainty about the mixture of single electrons coming from both B and D [22, 28, 29]), but within still larger uncertainties, even more for the first data coming from collisions at LHC [31]. A successful prediction at RHIC for both $R_{AA}(p_T)$ and $v_2(p_T)$ was achieved by including non-perturbative contributions [17] from the quasi-hadronic bound state describe above. However the uncertainty in establishing the strength of the non-perturbative effect and the fraction of B and D feed-down into single electron and the properties of the bulk dynamics employed [32] has not made possible to draw definitive conclusions. Furthermore also in a pQCD framework supplemented by Hard Thermal Loop (HTL) scheme several progress has been made evaluating realistic Debye mass and running coupling constants [18, 38], different models for the expansion of the QGP [32, 33] and three-body scattering effects [34, 37] have been implemented to improve the description of the data. In the upcoming future new data will be available at both RHIC and LHC. Such new data will have a better statistic and will extend to lower p_T and it will probably be possible to measure also the angular correlation between $c(b)$ and $\bar{c}(\bar{b})$ that will allow to have a better understanding of the HQ interaction at high temperature.

3. Boltzmann vs Fokker-Planck dynamics

The propagation of HQ in QGP has been quite often treated within the framework of Fokker-Planck equation [3, 7, 8, 9]. The main reason is that it was believed that their motion can be assimilated to a Brownian motion due to their perturbative interaction and large mass that should generically lead to collisions sufficiently forward peaked and/or with small momentum transfer. Under such constraints it is known that also the Boltzmann transport equation reduces to a Fokker-Planck dynamics [7], which constitutes a significant simplification of in medium dynamics. Such a scheme has been very widely employed including some of the authors [8, 9, 10, 17, 36, 32, 38, 11, 44, 45, 47, 46] in order to calculate the experimentally observed nuclear suppression factor (R_{AA}) [28, 29, 22, 31] and their large elliptic flow (v_2) [22] for the non-photonic single electron spectra.

Along with the Fokker-Planck approach in some work a description of HQ within a relativistic Boltzmann transport approach has been developed including both collisional and radiative energy loss [18, 57, 58]. The last appears within the data error bars to be more close to the possibility to predict simultaneously both R_{AA} and v_2 for $Pb + Pb$ at $\sqrt{s} = 2.76$ ATeV. Also other authors have in the past and more recently undertaken the study of charm quarks within a Boltzmann approach [40, 41, 42, 43].

To clarify the possible differences that may come from a Fokker-Planck description respect to a solution of the Boltzmann collision integral, we discussed in this talk in quite some detail the similarities and differences between the two approaches. This is a first study trying to understand if there can be some ambiguity in the data interpretation coming from differences in the two transport approaches currently employed to investigate the phenomenology of open heavy flavor in ultra-relativistic HIC. Indeed the motivation of employing a Fokker-Planck approach were initially more related to the prejudice that the momentum transfer suffered by HQ is small for both charm and bottom quarks. On the other hand, a suppression factor R_{AA} and v_2 similar for light and heavy

flavors, observed experimentally, rise the suspect that the momentum transfer may not be really sufficiently small. Therefore we study the impact of the approximations involved by Fokker-Planck equation by mean of a direct comparison with the full collisional integral within the framework of Boltzmann transport equation. The study has been firstly conducted comparing Boltzmann and Fokker-Planck dynamics in a box bulk medium at fixed temperature, which allows a better assessment of the underlying dynamics providing a solid basis for understanding the more complex HIC dynamics. Before we briefly review the main ingredients of the two transport equations.

The Boltzmann equation for the HQ distribution function can be written in a compact form as:

$$p^\mu \partial_\mu f_Q(x, p) = \mathcal{C}[f_Q](x, p) \quad (3.1)$$

where $\mathcal{C}[f_Q](x, p)$ is the relativistic Boltzmann-like collision integral where the phase-space distribution function of the bulk medium appears as an integrated quantity in $\mathcal{C}[f_Q]$, see for example Ref.s [54, 55], while we are interested to the evolution of the heavy quarks distribution function $f_Q(x, p)$. The distribution function of the bulk medium has in general to be determined by another set of equations that could be the Boltzmann-Vlasov equation for quark and gluons or the hydrodynamics equations. In our study the bulk medium will be just a thermal bath at some temperature T , which allows to better test and compare the dynamics of HQ in a Boltzmann transport dynamics respect to a Fokker-Planck one. This an intermediate step before studying the more complex case of the expanding medium in uRHIC that we will discuss at the end of the talk.

For the purpose of focusing on the momentum transferred in the collisions the relativistic collision integral can be written in a simplified form [3, 7] in the following way:

$$\mathcal{C}[f_Q](x, p) = \int d^3k [\omega(p+k, k) f_Q(x, p+k) - \omega(p, k) f_Q(x, p)] \quad (3.2)$$

where $\omega(p, k)$ express the collision rate of heavy quark per unit of momentum phase space which changes the heavy quark momentum from p to $p-k$, with the first term in the integrand being the gain of probability through collisions and the second term the loss out of that momentum space volume. HQ interact with the medium by mean of two-body collisions regulated by the scattering matrix of the process $g+Q \rightarrow g+Q$ ($\sigma_{g+Q \rightarrow g+Q}$), therefore defining the relative velocity between the two colliding particles as v_{rel} the transition rate can be written as:

$$\omega(p, k) = \int \frac{d^3q}{(2\pi)^3} f_g(x, p) v_{rel} \frac{d\sigma_{g+Q \rightarrow g+Q}}{d\Omega} \quad (3.3)$$

where $\sigma_{g+Q \rightarrow g+Q}$ is related to the scattering matrix $|\mathcal{M}_{gQ}|^2$:

$$v_{rel} \frac{d\sigma_{g+Q \rightarrow g+Q}}{d\Omega} = \frac{1}{d_c} \frac{1}{4E_p E_q} \frac{|\mathcal{M}_{gQ}|^2}{16\pi^2 E_{p-k} E_{q+k}} \delta^0(E_p + E_q - E_{p-k} - E_{q+k}) \quad (3.4)$$

We recall that the scattering matrix is the real kernel of the dynamical evolution for both the Boltzmann approach and the Fokker-Planck one. Of course all the calculations discussed in the following will originate from the same scattering matrix for both cases.

The Boltzmann equation is solved numerically dividing the space into a three-dimensional lattice and using the test particle method to sample the distributions functions. The collision integral is solved by mean of a stochastic implementation of the collision probability $P = v_{rel} \sigma_{g+Q \rightarrow g+Q}$.

$\Delta t/\Delta x$ [51, 52, 54, 56]. The code has been widely tested as regard the collision rate and the evolution of non-equilibrium initial distributions toward the Boltzmann-Juttner equilibrium distribution both as a function of cross section, temperature and mass of the particles, including non-elastic collisions [53].

3.1 Heavy quark momentum evolution in Langevin dynamics

The non-linear integer-differential Boltzmann equation can be significantly simplified employing the Landau approximation whose physical relevance can be associated to the dominance of soft scatterings with small momentum transfer $|\mathbf{k}|$ respect to the particle momentum \mathbf{p} . Namely one expands $\omega(p+k, k)f(x, p+k)$ around k ,

$$\omega(p+k, k)f_Q(x, p+k) \approx \omega(p, k)f(x, p) + k \frac{\partial}{\partial p}(\omega f) + \frac{1}{2} k_i k_j \frac{\partial^2}{\partial p_i \partial p_j}(\omega f) \quad (3.5)$$

Inserting Eq.(3.5) into the Boltzmann collision integral, Eq.(3.2), one obtains the Fokker Planck Equation:

$$\frac{\partial f}{\partial t} = \frac{\partial}{\partial p_i} \left[A_i(\mathbf{p})f + \frac{\partial}{\partial p_j} [B_{ij}(\mathbf{p})] \right] \quad (3.6)$$

by simply defining $A_i = \int d^3k w(\mathbf{p}, \mathbf{k})k_i = A(\mathbf{p})p_i$ and $B_{ij} = \int d^3k w(\mathbf{p}, \mathbf{k})k_i k_j$ that are directly related to the so called drag and diffusion coefficient. The Fokker-Planck equation can be solved by a stochastic differential equation i.e the Langevin equation, can be written as [3, 9, 11]:

$$\begin{aligned} dx_i &= \frac{p_i}{E} dt, \\ dp_i &= -A p_i dt + (\sqrt{2B_0} P_{ij}^\perp + \sqrt{2B_1} P_{ij}^\parallel) \rho_j \sqrt{dt} \end{aligned} \quad (3.7)$$

where dx_i and dp_i are the coordinate and momentum changes in each time step dt . A is the drag force and B the longitudinal and transverse diffusions, ρ is a stochastic variable Gaussian distributed. in terms of independent Gaussian-normal distributed random variables ρ_j , and

$$P_{ij}^\perp = \delta_{ij} - \frac{p_i p_j}{p^2}, P_{ij}^\parallel = \frac{p_i p_j}{p^2}. \quad (3.8)$$

are the transverse and longitudinal tensor projectors. We will employ the common assumption, $B_0 = B_1 = D$ [9, 10, 11, 17, 18, 37, 44]. To achieve the equilibrium distribution $f_{eq} = e^{-E/T}$ with $E = \sqrt{p^2 + m^2}$ as the final distribution one need to adjust the drag coefficient A in accordance with the Einstein relation [48] (see also [50])

$$A(p) = \frac{D(p)}{ET} - \frac{D'(p)}{p}. \quad (3.9)$$

We have checked that if the drag A and diffusion D coefficients are related by the fluctuation-dissipation theorem (FDT) the distribution function $f(\mathbf{p})$ converges to the Boltzmann-Juttner function $e^{-E/T}$. However when the A and D are directly calculated from the scattering matrix \mathcal{M}_{gc} it is not guaranteed that they fulfill the FDT because the Fokker-Planck equation is just a projection of the effect of scattering into first (drag) and second (diffusion) moments and it cannot be guaranteed that the dynamics implied by the scattering processes can be fully encased into a momentum shift plus a Gaussian fluctuations around the average momentum. However we have checked that generally for all the cases considered the violation of the FDT is marginal at least for momenta $p \gtrsim 1.5\text{GeV}$ that is the region of interest for our following discussion.

4. Scattering Matrix, cross section and Drag-Diffusion coefficients

The elastic collisions of heavy quarks with the gluon in the bulk has been considered within the framework of pQCD. The expression of the scattering matrix \mathcal{M}_{gQ} is the well known Combridge matrix that includes s, t, u channel and their interferences terms, augmented with a screening mass $m_D = g(T)T$ inspired by the HTL scheme as detailed in the Appendix. We have taken a charm quark mass $m_c = 1.3 \text{ GeV}$ and a bottom quark mass $m_b = 4.2 \text{ GeV}$. Our purpose is to perform the comparison between the Langevin and Boltzmann transport equations for different momentum transfer scenario that can be directly related to the angular distribution of scattering matrix or cross section. This can be achieved by using three different values of the Debye screening masses (m_D) needed to shield the divergence associated with the t-channel of the scattering matrix. As well known a small screening mass corresponds to forward peaked differential cross section, as we show in Fig.4 (left) by solid lines for charm quarks and dashed lines for bottom quarks. We have chosen three values for m_D , one is 0.83 GeV that corresponds to $m_D = \sqrt{4\pi\alpha_s} T$ with $\alpha_s = 0.35$ at $T = 400 \text{ MeV}$ that is the main temperature we will consider for our study. The other two values correspond to a reduction factor of two ($m_D = 0.4 \text{ GeV}$) and an increase of a factor of two ($m_D = 1.6 \text{ GeV}$). We can see in Fig.4 that $m_D = 0.4 \text{ GeV}$ corresponds to a situation where the scattering is quite forward peaked and $m_D = 1.6 \text{ GeV}$ instead corresponds to a situation where the scatterings are nearly isotropic, see Fig. 4 and Ref.[49]. We mention that the last is an artificial way to get close to physical situation in which one predict the existence of resonant states that corresponds isotropic scatterings [10, 17, 47].

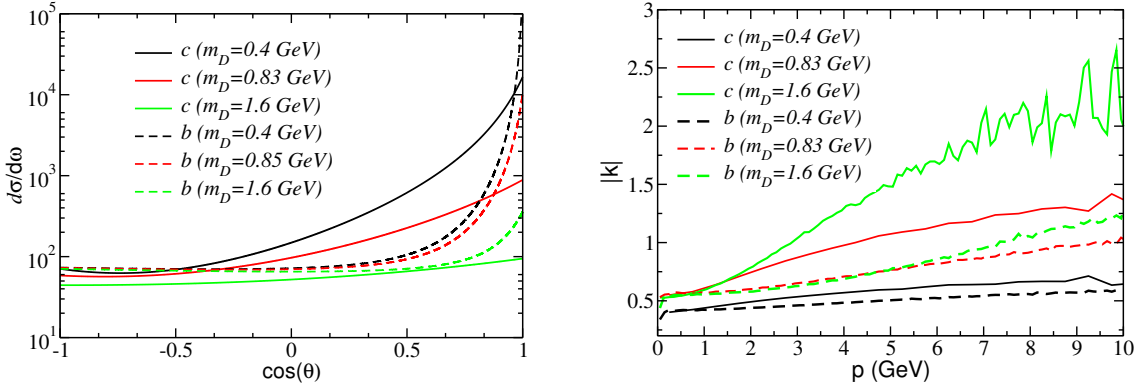


Figure 4: Right: Angular dependence of the cross section for different values of m_D for charm quarks (solid lines) and for bottom quarks (dashed lines); Left: variation of momentum transfer with p for different values of m_D for charm quarks (solid lines) and for bottom quarks (dashed lines).

In Fig.4 (right) we show the momentum transfer corresponding to the different angular distribution or different values of m_D for both charm (solid lines) and bottom (dashed lines) quarks as a function of the HQ momentum P when the bulk medium is at a temperature $T = 400 \text{ GeV}$. For an HQ momentum $|\mathbf{p}| = 5 \text{ GeV}$ we see that one goes from a momentum transfer $|\mathbf{k}| = 0.5 \text{ GeV}$ for the forward peaked scattering matrix corresponding to $m_D = 0.4 \text{ GeV}$ to a $|\mathbf{k}| = 1.5 \text{ GeV}$ for the nearly isotropic cross section corresponding to $m_D = 1.6 \text{ GeV}$. For bottom quarks, due to their

larger mass corresponding to $M_{bottom}/T \sim 10$ the change is less pronounced and indeed also for nearly isotropic cross sections is at most about 0.8 GeV which means about a factor 4 smaller than the bottom mass.

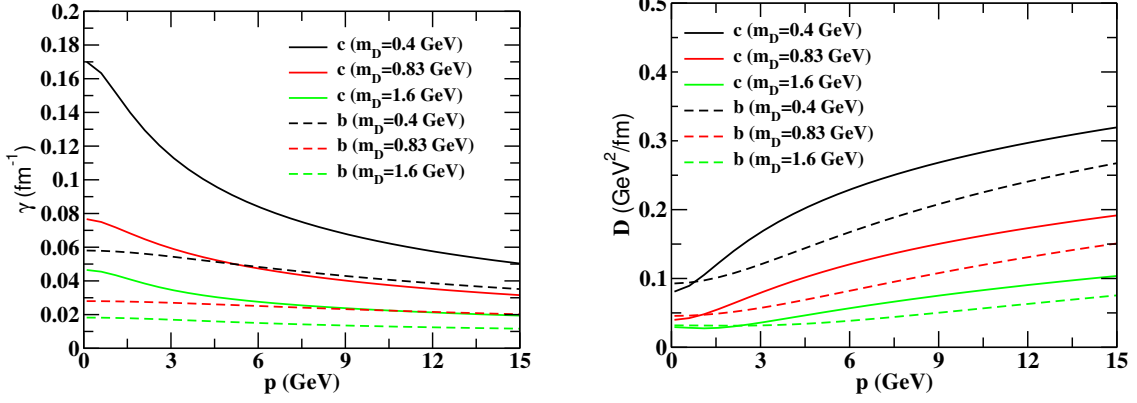


Figure 5: Left: Drag coefficients vs p at $T = 400$ MeV for different values of m_D ; Right: diffusion coefficients vs p at $T = 400$ MeV for different values of m_D .

Starting from the same scattering matrix \mathcal{M}_{gQ} we have evaluated the Drag $A(p)$ and Diffusion constant $B(p)$ that enter in Langevin equation, see Eq. 3.6. The result are shown in Fig.s 5 for both charm (solid lines) and bottom (dashed lines) quarks.

In order to have a similar R_{AA} within the typical time scale of uRHIC $\tau \approx 4 - 8$ fm/c we have multiplied by k factor the \mathcal{M}_{gQ} that has been chosen to be $k = 2.1$ for $m_d = 0.4$ GeV, $k = 4$ for $m_D = 0.83$ GeV and $k = 7.2$ for $m_D = 1.6$ GeV [57]. However the effect discussed does not depend on such k factor that has been included to set similar time scales and evolution of the spectra ($R_{AA}(p_T)$) reaching spectra evolution similar to that observed in HIC at RHIC and LHC which means $R_{AA}(p) \sim 0.3$ at momenta of about 4 – 6 GeV. However there is no necessity to set them exactly equal because we are interested only in comparing the Fokker-Planck and Boltzmann evolution starting from the same kernel given by the scattering matrix.

5. Numerical results: comparing the Boltzmann and Langevin evolution

We now discuss the evolution of momentum distributions of charm and bottom quarks interacting with a bulk medium at $T = 0.4$ GeV with scattering processes determined by the scattering matrices discussed in the previous section. The initial distribution of heavy quarks are taken from Ref. [59] and given by $f(p, t = 0) = (a + bp)^{-n}$ with $a = 0.70$ (57.74), $b = 0.09$ (1.00) and $n = 15.44$ (5.04) for charm and bottom quarks respectively. The above function give a reasonable description of D and B meson spectra in the p-p collision at highest RHIC energy. Our purpose is to compare the time evolution starting from the same initial momentum distribution and evaluating in each case considered both the differential cross section $d\sigma/d\Omega$, main ingredient of the Boltzmann equation, and the drag and diffusion coefficient, key ingredient of the Langevin equation both originating by the same scattering matrix.

We have plotted the results as a ratio between Langevin to Boltzmann at different times to quantify how much the ratio deviates from 1. We started the simulation at $t = 0$ fm/c which of course corresponds to a ratio of 1 as we start the simulation with the same initial momentum distribution for both Langevin and Boltzmann equations. So any deviation from 1 would reflect how much the Langevin differ from the Boltzmann evolution.

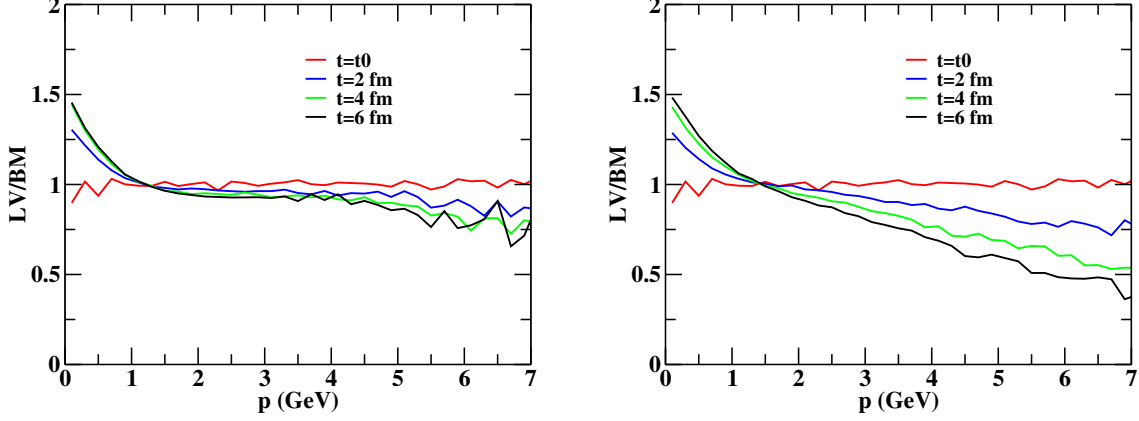


Figure 6: Left: Ratio between the Langevin (LV) and Boltzmann (BM) p_T -spectra for charm quark as a function of momentum for $m_D = 0.83$ GeV at different time; Right: ratio between the Langevin (LV) and Boltzmann (BM) spectra for charm quark as a function of momentum for $m_D = 0.4$ GeV at different time.

In Fig 6 the ratio of Langevin to Boltzmann spectra for the charm quark for $m_D = 0.4$ GeV (left) $m_D = 0.83$ GeV (right) has been displayed as a function of momentum at different time. We remind that time scales of 4–6 fm/c can be roughly taken as those corresponding to typical lifetime of a QGP in uRHIC's. This is why we are displaying and discussing the results around such time. We see that for the smaller screening mass corresponding to more forward peaked cross section the differences between Langevin and Boltzmann are quite limited and small than a 15%. Instead for $m_D = 0.83$ GeV it is observed that for $t = 4$ fm/c a deviation of Langevin from Boltzmann is around 40% and for $t = 6$ fm the deviation is around a 50% at $p = 5$ GeV, which suggests Langevin approach overestimates the average energy loss considerably due to approximation it involves.

When we consider a larger screening mass, $m_D = 1.6$ GeV to simulate a nearly isotropic scattering, the transferred momentum is about a factor of three larger and we see that the ratio of Langevin to Boltzmann spectra in Fig 7 at different time can lead to differences as large as a factor 75% at $t=4$ fm/c. It is however also to consider that for this last case the results depends on the procedure chosen to determine the Drag $A(p)$ and Diffusion coefficients $D(p)$. However just for this case if one calculates the diffusion coefficient from the scattering matrix and the drag one from the constraint of the fluctuation dissipation theorem (FDT) the result are significantly modified. In particular the LV/BM ratio will evolve quite slowly and the ratio reaches value about $\sim 0.6 - 0.7$ at $t=4$ fm/c. Such ambiguity in determining the drag and diffusion coefficient is much less relevant for the case of smaller m_D , however it essentially means that for nearly isotropic scatterings associated to large momentum transfer the dynamics of the scattering cannot be really encased into a simply shift of the average momenta with a Gaussian diffusion round such a mean and this manifest into a

stronger breaking of the FDT when both drag and diffusion are evaluated from \mathcal{M}_{gQ} .

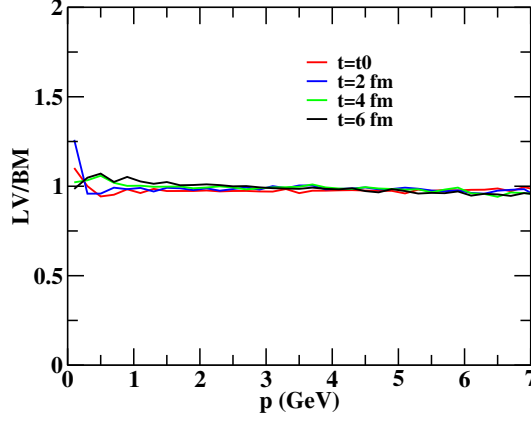


Figure 7: Ratio between the Langevin (LV) and Boltzmann (BM) spectra for bottom quark as a function of momentum for $m_D = 0.83$ GeV at different time;

We now move to the calculation for bottom quarks. In Fig. 8 the results for bottom quark are displayed for $m_D = 0.83$ GeV, results for the other two values of m_D are quite similar. It is observed that the ratio stays practically almost unity for bottom quark at all the time considered in the manuscript. Therefore, for bottom quark the Langevin approach is really a good approximation of Boltzmann equation independently of the angular dependence of the scatterings, at most a 10% difference is observed for $m_D = 1.6$ GeV. On the other hand as already observed due to the large bottom mass an approximation of the dynamics to a Brownian motion appears always appropriate. We notice that this is determined by the ratio of the mass and the temperature that determines the average momentum of the particles colliding with heavy quarks ($\langle p \rangle \simeq 3T$). For the charm quark $M_c/T \simeq 3$ while for bottom quark $M_b/T \simeq 10$ for the temperature we are considering.

5.1 Momentum spread of heavy quarks

A more thorough investigation of the different heavy quark evolution implied by a Langevin and a Boltzmann approach, we study the heavy quark momentum evolution considering the initial charm and bottom quark distribution as a delta distribution at $p = 10$ GeV for the the case with $m_D = 0.83$ GeV. The momentum evolution of the charm quarks are displayed in Fig. 9 within the Langevin dynamics. It is observed that both the charm and bottom quarks are Gaussian distribution as expected by construction. This present calculation reveals that the equilibrium distribution can be achieved at the end of the evolution by implementing the FDT but their dynamical evolution is quite different for charm quarks. As known the Langevin dynamics consists of a shift of the average momenta with a fluctuation around such a value that includes also the possibility to gain energy for the HQ as we see from the tail of the momentum distribution that overshoots the initial momentum $p = 10$ GeV at $t = 2$ fm/c, black solid line in Fig.9.

In Fig. 10 we present the momentum distribution for charm quark within the Boltzmann equation, is evident a very different evolution of the particles momentum which does not have a Gaussian shape and already at $t = 2$ fm/c has a very different spread in momentum with a larger contribution from processes where the charm can gain energy and a long tail at low momenta corresponding

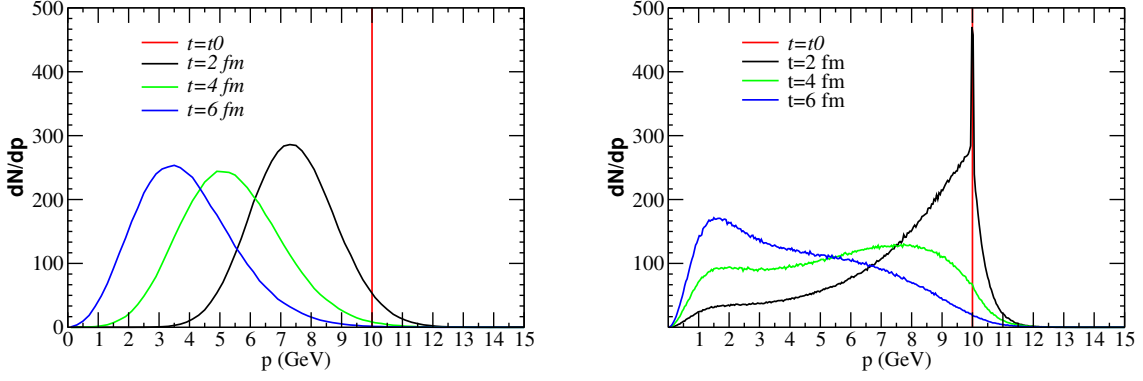


Figure 8: Evolution of charm quark momentum distribution within Langevin dynamics (left) and Boltzmann equation (right) considering the initial momentum distribution of the charm quarks as a delta distribution at $p=10$ GeV.

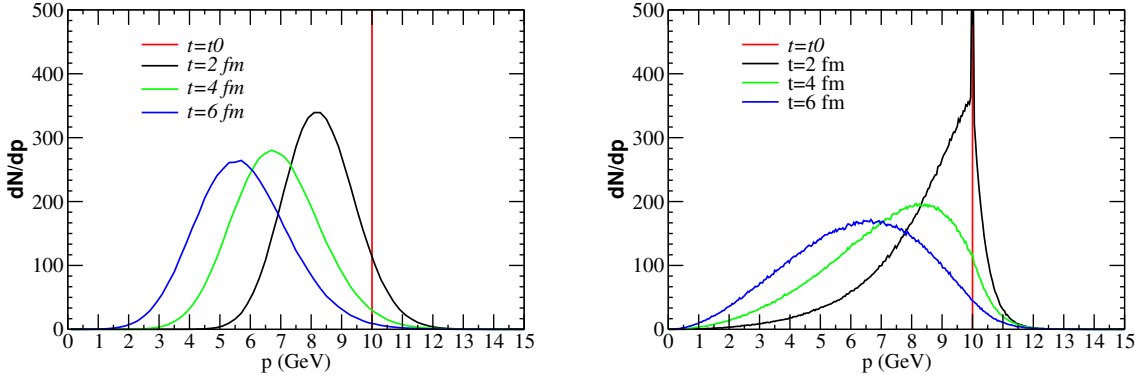


Figure 9: Evolution of bottom quark momentum distribution within Langevin dynamical (left panel) and the Boltzmann (right panel) considering the initial momentum distribution of the bottom quark as a delta distribution at $p=10$ GeV.

to some probability to loose a quite large amount of energy and in general a global shape that is not a at all of Gaussian form. This essentially indicates that for a particle with $M \sim \langle p \rangle \sim 3T$ as it is for the charm at a temperature $T = 0.4$ GeV the evolution is not of Brownian type. For the bottom quarks, shown in Fig. 9, the momentum evolution gives a much better agreement between the Boltzmann and the Langevin evolution because $M_{bottom}/T \simeq 10$. We notice that in figure 9 we have plotted the momentum distribution at larger time steps t_i respect to the figures at 400 MeV. This Because the drag coefficient A is about a factor three smaller. Therefore we have chosen to plot the distribution at time steps such that $t_i A$ is almost the same as in the previous figures 8,9. However even in the bottom case at $T = 0.4$ GeV ($M_{bottom}/T \simeq 10$) while the evolution of the global spectra are practically identical between the Langevin and Boltzmann dynamics, see Fig.8, the detail of the energy loss of a single bottom quark remains still significantly different. The momentum

distribution is reminiscent of a Gaussian distribution showing clearly a peak around the average momentum but still it has an asymmetric distribution with a longer tail towards lower momenta.

It would be interesting to study to find observables that are sensitive to such details of the HQ dynamics. A first candidate could be the $D\bar{D}$ and/or $B\bar{B}$ correlation [60] that should be quite different in a Langevin dynamics respect to the Boltzmann one since the momentum evolution of a single quark is so different, in particular for charms quarks. For the charm quark the very different change in momenta could determine also a quite different dynamics for the suppression of charmonium in medium.

5.2 Time Evolution of the Nuclear Modification factor R_{AA}

One of the key observable, investigated at RHIC and LHC energies, is the depletion of high p_T particles (D and B mesons or single e^\pm) produced in heavy-ion collisions with respect to those produced in pp collisions. Therefore we conclude our analysis showing the evolution of the spectra in terms of the $R_{AA}(p_T)$ for charm quarks evolving according to the LV and BM transport equations. We calculate the nuclear suppression factor, R_{AA} , using our initial $t = 0$ and final $t = t_f$ charm quark distribution as $R_{AA}(p) = \frac{f(p,t_f)}{f(p,t_0)}$.

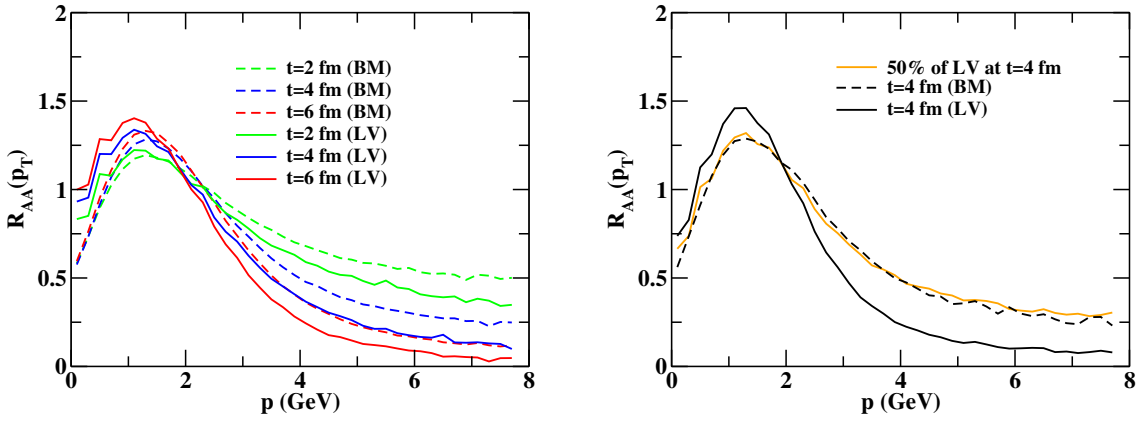


Figure 10: Left: the nuclear suppression factor, R_{AA} as a function of momentum from the Langevin (LV) equation and Boltzmann (BM) equation for charm quark in a box at $T=0.4$ GeV and $m_D = 0.83$ GeV; Right: the nuclear suppression factor, R_{AA} as a function of momentum from the Langevin (LV) equation and Boltzmann (BM) equation for charm quark in a box at $T=0.4$ GeV and $m_D = 1.6$ GeV. The orange line is the LV with a Drag and Diffusion coefficients reduced by 50%.

The nuclear suppression factor, R_{AA} , has been displayed in Fig 10 as a function of momentum from both Langevin and Boltzmann side at different time for $m_D = 0.83$ GeV. From Fig 10 we see that the time evolution of the nuclear suppression factor differ substantially from Langevin to Boltzmann comparing them at the same time. Similar trends are seen also at $m_D = 0.4$ GeV but with a much smaller deviation of the order of 15% while at $m_D = 1.6$ GeV the deviation in the time evolution are even larger. Since the diffusion coefficient is the important quantity for the phenomenological study, it is more meaningful from a phenomenological point of view to evaluate how much we need to change the diffusion coefficient/interaction from Langevin side to reproduce

the same nuclear suppression factor of Boltzmann equation. We find for the case $m_D = 1.6 \text{ GeV}$ in Fig. 10 (right) that we need to reduce the diffusion coefficients of Langevin equation by 50% to get similar nuclear suppression factor as of Boltzmann equation at the same time $t = 4 \text{ fm/c}$ which is the typical life time of the system produced at RHIC and anyway the time at which we have an $R_{AA}(p_T)$ quite similar to the one observed at RHIC and LHC in semi central collisions. For the case of $m_D = 1.6 \text{ GeV}$ it is enough to have a 30% reduction. We do not display also the experimental data because we are simply study the evolution of R_{AA} in a box at fixed T .

Our main aim here was simply to show that even if the underlying dynamics of the charm quark can be quite different between the LV and the BM transport approaches at the level of the $R_{AA}(p_T)$. One can anyway mimic the same result mocking the differences in the dynamical evolution by modifying the interaction by an amount that can go from about a 10% up to about a 50% depending on the angular dependence of the scatterings that entail the strength of the transferred momentum. We have not shown results for the bottom case because in the first part of this section we do not observe significant difference in the time evolution of the spectra between the LV and BM descriptions.

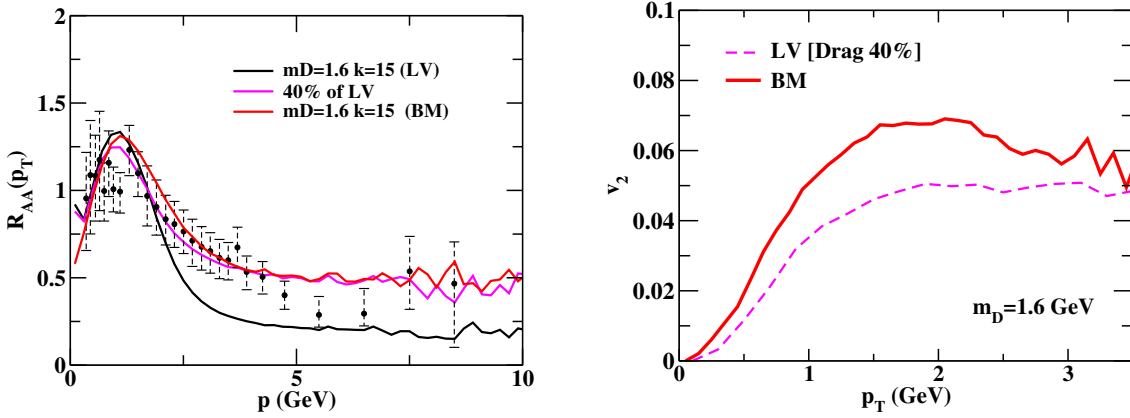


Figure 11: The nuclear suppression factor, R_{AA} as a function of momentum p_T from the Langevin (LV) equation and Boltzmann (BM) equation for charm quark in a box at $T=0.4 \text{ GeV}$ and $m_D = 1.6 \text{ GeV}$

Finally we show a first preliminary result for the case of a realistic simulation of $Au + Au$ collisions at $\sqrt{s_{NN}} = 200 \text{ GeV}$. In Fig.11 (left) we compare the result of a Langevin and a Boltzmann approach for the case $m_D = 1.6 \text{ GeV}$ with the experimental data (full circles) from PHENIX Collaboration for the single electron coming from the semileptonic decay of B and D mesons. We see that the Langevin approach in this case predicts a much smaller $R_{AA}(p_T)$ respect to the Boltzmann one. However similarly to what has been seen in the box simulation described above such a difference can be composed by reducing by a 60% the Drag coefficient in the Langevin case. This in itself would mean that the use of Langevin can underestimated the Drag coefficient up to about a 50%, but even mre important is that even is one obtains the same $R_{AA}(p_T)$ the elliptic flow $v_2(p_T)$, shown in Fig.11 (left), is anyway quite larger in the Boltzmann case going toward the large v_2 observed experimentally.

6. Conclusions and Outlook

We have briefly review the interest for the Heavy Quark dynamics in the QGP. After recalling that charm and bottom quarks can be considered heavy because both m_Q/Λ_{QCD} and m_Q/T are much larger than unity. However a more closer look into the physics involved tells that there is another scale to be considered $m_Q / \langle p_{bulk} \rangle = m_Q/3T$. For this last scale the charm cannot be considered really heavy at $T \gtrsim 300$ MeV. In fact comparing the momentum evolution of a charm quark solving the full Boltzmann integral shows a dynamical evolution that appear to be quite far from a Brownian motion. This can lead to underestimate the charm quark drag coefficient and furthermore to under estimate the build-up of elliptic flow $v_2(p_T)$. The strength of the effect depends however on the details of the angular distribution of the scattering process and become relevant only if the the differential cross section is not very forward peaked.

References

- [1] E. V. Shuryak, Nucl. Phys. A **750** (2005) 64
- [2] B. V. Jacak and B. Muller, *Science* **337**, 310 (2012).
- [3] R.Rapp and H van Hees, R. C. Hwa, X. N. Wang (Ed.) Quark Gluon Plasma 4, 2010, *World Scientific*, **111** [arXiv:0903.1096 [hep-ph]]
- [4] M. Cacciari, P. Nason and R. Vogt, Phys. Rev. Lett. **95** (2005) 122001
- [5] M. Cacciari, S. Frixione, N. Houdeau, M. L. Mangano, P. Nason and G. Ridolfi, JHEP **1210** (2012) 137
- [6] F. Antinori, J. Phys. G **30** (2004) S725 [nucl-ex/0404032].
- [7] B. Svetitsky, Phys. Rev. D **37**, 2484 (1988)
- [8] M.G. Mustafa, D. Pal and D. K. Srivastava, Phys. Rev. C **57**, 889 (1998)
- [9] G. D. Moore, D Teaney, Phys. Rev. C **71**, 064904 (2005)
- [10] Hees H van, Greco V and Rapp R 2006 *Phys. Rev. C* **73**, 034913
- [11] S. Cao, S. A. Bass, Phys. Rev. C **84**, 064902 (2011)
- [12] M. Djordjevic, M. Gyulassy, R. Vogt and S. Wicks, Phys. Lett. B **632** (2006) 81
- [13] N. Armesto, M. Cacciari, A. Dainese, C. A. Salgado and U. A. Wiedemann, Phys. Lett. B **637** (2006) 362
- [14] S. Batsouli, S. Kelly, M. Gyulassy and J. L. Nagle, Phys. Lett. B **557** (2003) 26
- [15] V. Greco, C. M. Ko and R. Rapp, Phys. Lett. B **595** (2004) 202
- [16] P. Petreczky and K. Petrov, Phys. Rev. D **70**, 054503 (2004)
- [17] H. Van Hees, M. Mannarelli, V. Greco and R. Rapp, Phys. Rev. Lett. **100**,192301 (2008)
- [18] P. B. Gossiaux, J. Aichelin, Phys. Rev. C **78** 014904 (2008); P.B. Gossiaux, J. Aichelin, T. Gousset and V. Guiho, J. Phys. G **37**, 094019 (2010)
- [19] M. Asakawa, T. Hatsuda, Phys. Rev. Lett. **92**, 012001 (2004), Nucl. Phys. A**721**, 869 (2003).
- [20] O. Kaczmarek, F. Karsch, P. Petreczky, and F. Zantow, Nucl.Phys.Proc.Suppl. **129**, 560 (2004)

- [21] O. Kaczmarek and F. Zantow (2005), arXiv:hep-lat/0506019
- [22] A. Adare *et al.* (PHENIX Collaboration), Phys. Rev. Lett. **98**, 172301 (2007).
- [23] M. Mannarelli and R. Rapp, Phys. Rev. C **72**, 064905 (2005)
- [24] E. V. Shuryak and I. Zahed, Phys. Rev. D **70**, 054507 (2004)
- [25] M. Döring *et al.*, Phys. Rev. D **75**, 054504 (2007). [arXiv:hep-lat/0702009].
- [26] V. Greco, C. M. Ko and P. Levai, Phys. Rev. C **68** (2003) 034904 [nucl-th/0305024].
- [27] R. J. Fries, V. Greco and P. Sorensen, Ann. Rev. Nucl. Part. Sci. **58** (2008) 177 [arXiv:0807.4939 [nucl-th]].
- [28] B. I. Abeleb *et al.* (STAR Collaboration), Phys. Rev. Lett. **98**, 192301 (2007).
- [29] A. Adare *et al.* (PHENIX Collaboration), Phys. Rev. Lett. **98**, 172301 (2007)
- [30] F. Scardina, M. Di Toro and V. Greco, Phys. Rev. C **82** (2010) 054901.
- [31] B. Abelev *et al.*, (ALICE Collaboration) JHEP **1209** (2012) 112
- [32] P. B. Gossiaux *et al.*, arXiv:1102.1114 [hep-ph]
- [33] P. B. Gossiaux, J. Aichelin, M. Bluhm, T. Gousset, M. Nahrgang, S. Vogel and K. Werner, PoS QNP **2012** (2012) 160 [arXiv:1207.5445 [hep-ph]]
- [34] C. M. Ko and W. Liu, Nucl. Phys. A **783**, 23c (2007).
- [35] V. Greco, C. M. Ko and P. Levai, Phys. Rev. Lett. **90** (2003) 202302; V. Greco, C. M. Ko and P. Levai, Phys. Rev. C **68** (2003) 034904
- [36] Y. Akamatsu, T. Hatsuda and T. Hirano, Phys. Rev. C **79**, 054907 (2009)
- [37] S. K Das, J. Alam and P. Mohanty, Phys. Rev. C **82**, 014908 (2010); S. Majumdar, T. Bhattacharyya, J. Alam and S. K. Das, Phys. Rev. C **84**, 044901 (2012)
- [38] W. M. Alberico *et al.*, Eur. Phys. J. C, **71** 1666 (2011); W. M. Alberico *et al.*, Eur. Phys. J. C **73** 2481 (2013)
- [39] C. Young, B. Schenke, S. Jeon and C. Gale, Phys. Rev. C **86**, 034905 (2012)
- [40] M. Younus, C. E. Coleman-Smith, S. A. Bass and D. K. Srivastava, arXiv:1309.1276 [nucl-th].
- [41] B. Zhang, L. -W. Chen and C. -M. Ko, Phys. Rev. C **72** (2005) 024906
- [42] D. Molnar, Eur. Phys. J. C **49** (2007) 181
- [43] S. K. Das, F. Scardina, S. Plumari and V. Greco, arXiv:1309.7930 [nucl-th]
- [44] T. Lang, H. van Hees, J. Steinheimer and M. Bleicher, arXiv:1208.1643 [hep-ph]
- [45] S. Cao, G-Y. Qin, S. A. Bass and B. M. Müller, Nucl. Phys. A **904**, 653c (2013)
- [46] Hao-jie Xu, Xin Dong, Li-juan Ruan, Qun Wang, Zhang-bu Xu, and Yi-fei Zhang, arXiv:1305.7302
- [47] M. He, R. J. Fries and R. Rapp, Phys. Rev. Lett. **110**, 112301 (2013)
- [48] D. B. Walton and J. Rafelski, Phys. Rev. Lett. **84**, 31 (2002)
- [49] S. K. Das, F. Scardina and V. Greco, arXiv:1312.6857 [nucl-th].
- [50] S. Majumdar, T. Bhattacharyya and J. Alam, arXiv:1305.6445 [nucl-th]

- [51] G. Ferini, M. Colonna, M. Di Toro and V. Greco, Phys. Lett. B, **670**,325 (2009); V. Greco, M. Colonna, M. Di Toro and G. Ferini, Progr. Part. Nucl. Phys. **62**, 562 (2009)
- [52] M. Ruggieri, F. Scardina, S. Plumari and V. Greco, Phys. Lett. B **727** (2013) 177
- [53] F. Scardina, M. Colonna, S. Plumari and V. Greco, Phys. Lett. B **724** (2013) 296
- [54] Z. Xu and C. Greiner, Phys. Rev. C **71**, 064901 (2005)
- [55] A. Lang, W. Cassing, U. Mosel, H.H. Reusch, and K. Werner, Journal of Computational Physics 106, 391 (1993)
- [56] A. Lang *et al.*, Jour. of Comp. Phys. **106**, 391 (1993)
- [57] J. Uphoff, O. Fochler, Z. Xu and C. Greiner, Phys. Rev. C, **84** 024908 (2011)
- [58] J. Uphoff, O. Fochler, Z. Xu and C. Greiner, Phys. Lett. B **717** (2012) 430
- [59] M. Cacciari, P. Nason, and R. Vogt, Phys. Rev. Lett. **95**, 122001 (2005)
- [60] X. Zhu and N. Xu and P. Zhuang, Phys. Rev. Lett. **100**, 152301 (2008)